Real Time Data Acquisition and Control of a Sensorless Wind Turbine Emulator Using Fuzzy Logic Theory and a Dspace Board

Mohammed Mokhtari*‡, Soufyane Benzaouia**, Smail Zouggar***, Nacer M'Sirdi****

*Mohammadia School of Engineers, Mohammed V University in Rabat, Engineering for Smart and Sustainable Systems Research Center, Av. Ibn Sina Rabat, Morocco.

**Capgemini Engineering, Direction Research & Innovation, F-31700 Blagnac, France.

*** High School of Technology, Electrical Engineering and Maintenance Research Laboratory, Complexe universitaire AlQods Oujda, Morocco.

**** Laboratoire d'Informatique et Systèmes LIS, CNRS UMR 6168. Dom. Univ. St Jrme, Av. Escadrille Normandie - Niemen 13397. Marseille Cedex 20. France.

(mokhtari@emi.ac.ma, soufyane.benzaouia@gmail.com, szouggar@gmail.com, msirdink@free.fr)

‡ Corresponding Author; Mohammed MOKHTARI, Tel: +212 648 719 764,

mokhtari@emi.ac.ma

Received: 16.09.2023 Accepted:24.12.2023

Abstract- This study introduces a real-time sensorless Wind Turbine Emulator (WTE) platform designed to evaluate different wind energy conversion technologies and enhance research on wind power generation in a laboratory environment. The WTE calculations are executed using a PC connected to a Dspace control board and can effectively replicate the dynamic torque produced using an actual turbine. The emulation is achieved by controlling the armature current of a DC motor through a Single Input Fuzzy Logic Controller and an IGBT DC/DC Boost converter. A supervision interface was also developed with ControlDesk software to allow real-time control and data acquisition. Furthermore, this research paper provides a comprehensive understanding of the wind turbine modeling, theoretical analyses, operational principles, and experimental test results that confirm the viability and efficiency of this approach.

Keywords Wind turbine emulator, DC motor, DC/DC boost converter, Dspace CP1104, current armature control, single input fuzzy logic controller.

1. Introduction

In the latter part of the 20th century, renewable energy has experienced a remarkably substantial growth worldwide [24]. As wind power is abundant, freely available, clean and has boundless potential, it has emerged as a vital solution to address the global energy crisis specially with the raising price of oil, safety issues of nuclear power and its ecological problems [25].

Applications based on wind power systems have shown an excellent prospective to produce electricity for isolated and remote sites [23]. Yet, prior to the deployment of any Wind Turbine (WT) system, it is essential to conduct a thorough evaluation of its steady state and dynamic performances in a laboratory environment. By doing so, potential issues that may arise during installation can be proactively addressed and mitigated. A wind turbine emulator serves then as a valuable asset for the development of wind energy conversion systems (WECS) which can eliminate the need for natural wind resources and a physical wind turbine.

During the previous few years, numerous research initiatives on WECS have been conducted. Some are based on Induction Motors (IM) [9-11], while others use Permanent

Magnet Synchronous Machines (PMSM) [12-15], and some even employ DC motors [1-5].

In [9], the authors described an experimental platform for evaluating different MPPT algorithms. The platform incorporates an IM controlled through cascaded low-pass and high-pass filters. In Reference [11], the authors also discuss the creation of an IM-based emulator with a closed-loop PI controller. They employed the V/f control method, known for its rapid dynamic response. However, even with this method, they couldn't eliminate the steady-state error at high-speed range. Reference [10] introduces an IM controlled by an IGBT inverter, serving as a WTE system. The control of the drive relies on direct measurement of the shaft torque and speed. The control strategy incorporates two closed loops using conventional PI regulators for speed and torque control.

There have been several attempts to replace the induction motor with a permanent magnet synchronous motor. In [12], the authors chose an emulator that relies on load torque dynamic compensation of a PMSM to replicate the dynamic behavior of a wind turbine. In references [14], the proposed emulators used a PMSM in conjunction with a voltage source converter to simulate torque oscillations resulting from wind shear. In [13] and [15], the authors employed the field-oriented vector technique to control the torque and speed of the PMSG-based emulator.

Otherwise, from a control perspective and in terms of implementation, a separately excited DC motor is considered more suitable compared to PMSM and IM [7][21]. In Reference [2], it was employed with a single-phase half-drive to regulate the armature current of the proposed emulator using a conventional PI regulator. In the study described in Reference [3], an armature-controlled DC motor driven by a micro-controller PIC16F877 and a discrete PI controller was used to create the WTE. In References [1][4][5][22], the proposed emulators rely on a PWM converter and a conventional PI regulator to control the armature current winding of a separately excited DC machine.

In all of the aforementioned works, researchers used the conventional PI controller and relied on standard practice that uses mechanical sensors to capture critical parameters such as rotational speed or mechanical torque. So as to improve the quality and effectiveness of the referenced research, this manuscript introduces significant advancements in two key aspects:

- Firstly, it proposes a sensorless wind turbine emulator based on the Luenberger Observer. This adjustment reduces the overall cost of the testing equipment and enhances its stability against measurement inaccuracies.
- Secondly, the use of a nonconventional SIFLC controller offers enhanced performance compared to PI controller since it reduces sensitivity to disturbances, system model uncertainties and parameters variation.

These contributions collectively demonstrate a potential to advance wind turbine emulation research and mark a departure from the conventional methods prevalent in the field as shown in Table 1.

Table 1. Comparison of various configurations for wind turbine emulator (WTE)

References	Emulator Structure		Required Mechanical Sensors	Model knowledge	
	Motor type	Converter type		Controller	Observer
[10]	Induction Motor	3 Phase IGBT Inverter	Torque Sensor Speed Sensor	Required (PI Controller)	No Observer used
[13]	PMSM	3 Phase IGBT Inverter	Speed Sensor	Required (PI Controller)	No Observer used
[1]	DC motor	Phase-controlled AC/DC converter	Speed Sensor	Required (PI Controller)	No Observer used
[2]	DC motor	Single-phase half-controlled drive	Speed Sensor	Required (PI Controller)	No Observer used
[3]	DC motor	DC/DC Converter	Torque Sensor Speed Sensor	Required (Discrete PI Controller)	No Observer used
[4]	DC motor	DC/DC Buck Converter	Speed Sensor	Required (PI Controller)	No Observer used
This work	DC motor	DC-DC Boost Converter	Not Required	Not Required (Fuzzy Logic Controller)	Luenberger Observer

The developed platform will also serve as a laboratory test bench for future research activities that explore various aspects of wind power system control technology, such as:

- Testing wind turbine pitch angle and crowbar limitations under power over-rating scenarios or during low voltage ride-through events.
- Modeling and analyzing torque oscillations arising from wind shear, dynamic effects of large turbine inertia, and tower shadow effects.
- Developing and testing Maximum Power Point Tracking (MPPT) strategies to optimize wind turbine efficiency.
- Investigating the seamless connection and disconnection of wind turbines to and from the grid.in voltage regulation and maximum power tracking of variable speed wind turbine.

Regarding the organization of this research paper: In Section II, we propose an analysis of the studied wind turbine model and characteristics. Then the proposed wind turbine emulator and its control strategy will be introduced in section III. To finally conclude in section IV with the results of the experimental tests.

2. Wind Turbine Model and Characteristics

To be able to incorporate the nonlinear characteristics of a realistic wind turbine in the implemented wind turbine model, the non-dimensional power coefficient curve (Cp) must be taken in consideration. Under the assumption of neglecting wind shear and tower shadow effects, the Cp curve varies with alterations in Tip-Speed Ratio (TSR) λ which can be determined using the following formula:

$$\lambda = \frac{R * \omega}{V} \tag{1}$$

Where R represents the rotor radius, ω the rotor speed and V the wind speed.

The relationship between Cp and λ was obtained from the literature [6] and is described by the following quadratic equation:

$$\begin{cases} C_{p1}(\lambda,\beta) = C_1\left(\frac{C_2}{\gamma} - C_3.\beta - C_4\right)e^{\frac{-C_5}{\gamma}} + C_6.\lambda \\ C_1 = 0.5176, C_2 = 116, C_3 = 0.4, \\ C_4 = 5, C_5 = 21, C_6 = 0.0068 \\ \frac{1}{\gamma} = \frac{1}{\lambda + 0.08\beta} - \frac{0.035}{\beta^3 + 1} \end{cases} \tag{2}$$

The output mechanical power is then provided by:

$$P_{aer} = C_p(\lambda).\frac{\rho.\pi.R^2.V^3}{2} \tag{3}$$

Where ρ is the air density.

Hence, the transmitted aerodynamic torque can be deduced as following [20]:

$$C_{aer} = \frac{P_{aer}}{\Omega_{turbine}} = C_p(\lambda)\frac{\rho.\pi.R^2.V^3}{2.\Omega_{turbine}} \tag{4}$$

Where $\Omega_{turbine}$ the mechanical rotation speed of the turbine (tr/min).

Fig.2 illustrates the block diagram of the implemented turbine model in Matlab/Simulink software and Fig.1 presents the Cp (λ) characteristics for different pitch angle values. Note that the highest Cp value, reaching 0.48, occurs at λ = 8.12.

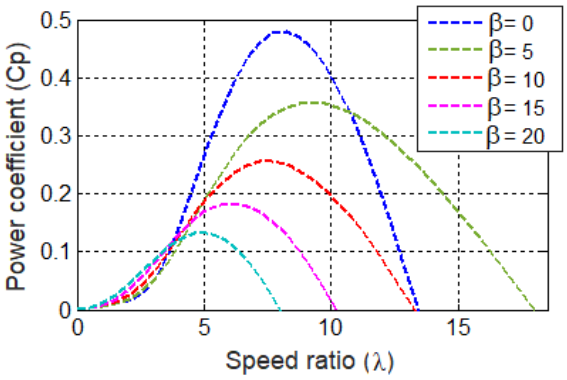


Fig. 1. Wind turbine characteristics.

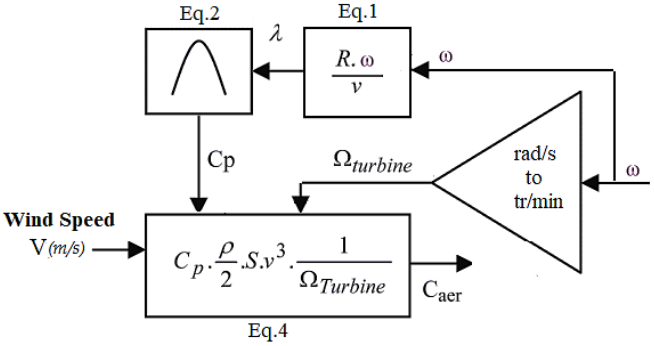


Fig. 2. Bloc diagram of the turbine model.

3. Wind Turbine Emulator

Considering the insights obtained from the literature review, a separately excited DC motor was selected as a solution to replicate the behavior of the studied WT. The armature current of the DC motor is controlled by a DC/DC boost configuration using a Dspace control board. The proposed hardware structure for the WTE is provided in Fig.3, where it can be observed that the emulator is mechanically linked to an AC generator as it will be in a real case of a WECS. The use of a gear box is mainly determined by the type of the chosen AC generator and is mandatory when the generator's nominal speed exceeds that of the turbine.

3.1. Control Strategy

To accurately replicate the authentic behavior of the WT using the DC machine, the identification of the armature current reference Ia_ref is essential. Knowing that the electromagnetic torque reference Cem_ref of the DC motor which we want to control is equal to the aerodynamic torque Caer derived from the turbine model. Ia_ref can then be

deduced from devising Cem_ref by torque constant Ki as indicated in Fig.4.

The closed-loop current controller performs a comparison between the measured armature current Ia and its reference value Ia_ref, if the error between the two is different of zero the Single Input Fuzzy Logic Controller (SIFLC) will adjust its output Alpha to control the DC/DC boost output voltage applied to the DC motor armature. Consequently, the fluctuation in the armature voltage will control the armature current based on the referenced current, leading the system to achieve a stable equilibrium.

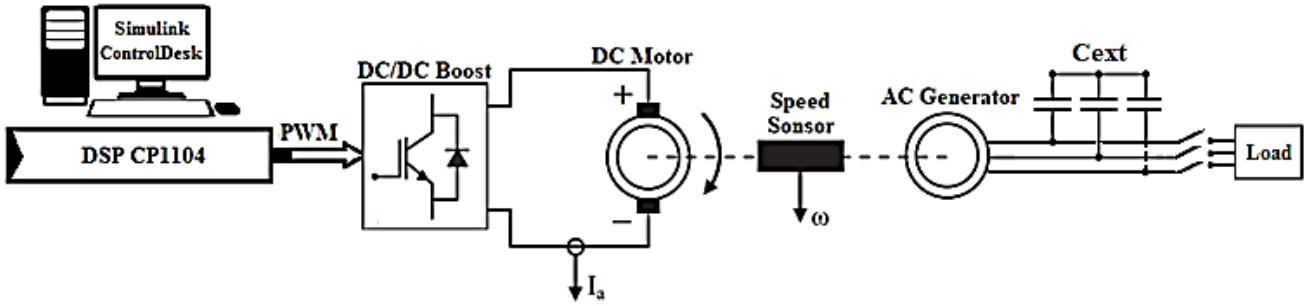


Fig. 3. Wind turbine emulator structure.

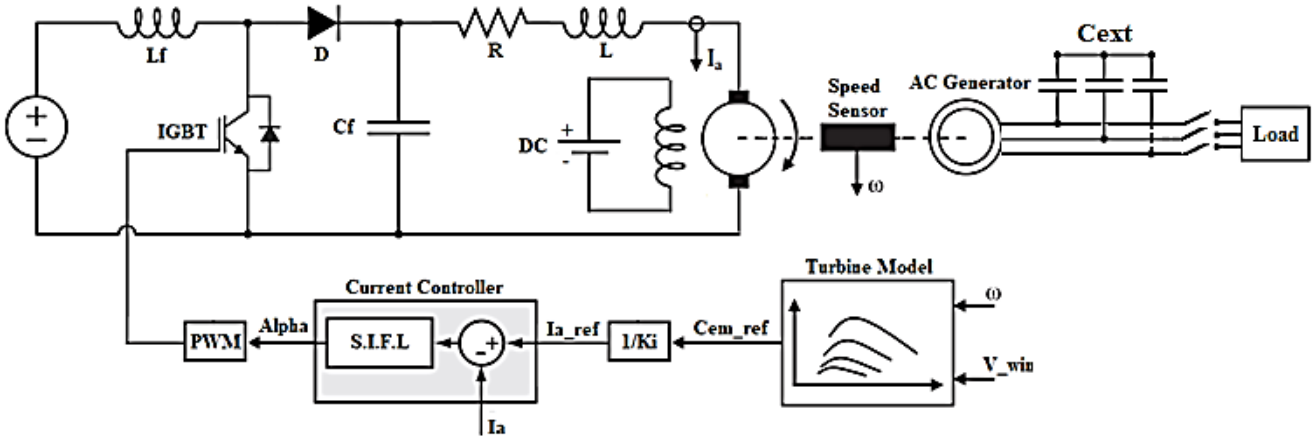


Fig. 4. Control scheme of the proposed wind turbine emulator.

The proposed single input fuzzy logic current controller utilized in this application offers several advantages. One notable benefit is its ability to operate with a single input variable, even when dealing with complex controlled plants [8]. This simplifies the control rule table and reduces the number of tuning parameters significantly. Consequently, defining membership functions, tuning rules, and scaling factors becomes much easier compared to standard Fuzzy Logic Controllers (FLCs) that rely on multiple input variables. As a result, the SIFLC provides a more straightforward approach to tuning the current controller while achieving the desired control performance [18].

The input signal for the SIFLC is the error between the measured DC motor armature current and its referenced current. The controller's output signal, on the other hand, is the value of dα [19].

The duty cycle value Alpha to be sent to the DSP CP1104 PWM circuit to produce the required gating pulses for driving the DC/DC boost IGBT is derived from adding the step change in the value of dα to the previous one. This technique is expressed using equation 5, illustrated in Fig.5 and described by the Flowchart in Fig.6:

$$\text{Alpha} = \sum \mathrm{d}\alpha(t) \tag{5}$$

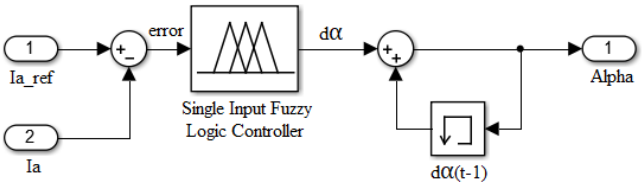


Fig. 5. Current controller structure.

- When the error is zero, indicating that the actual DC motor armature current Ia is equal to the reference current Ia_ref, the value of dα should be zero as well. This ensures that the value of α remains unchanged, preventing any alteration in the DC motor armature voltage.

- In the case of a negative error, where Ia surpasses the desired Ia_ref value, it is necessary to make a positive adjustment to α (dα). This adjustment results in an increase in α, which subsequently raises the armature voltage of the DC motor.

- In the event of a positive error, indicating that Ia falls below the desired Ia_ref value, it becomes necessary to make a negative adjustment to α (dα). This adjustment leads to a decrease in α, thereby reducing the armature voltage of the DC motor.

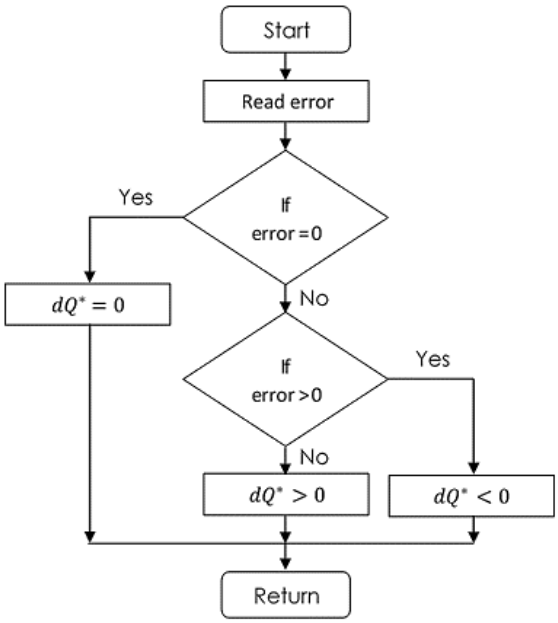


Fig. 6. Flowchart of the proposed control techniques.

In this work, the structure of the SIFLC is a Mamdani-type with five triangular rulebased-membership functions. The calculation of the controller output during the defuzzification process is based on the center of gravity. Fig.7 presents the input and output membership functions of the suggested SIFLC.

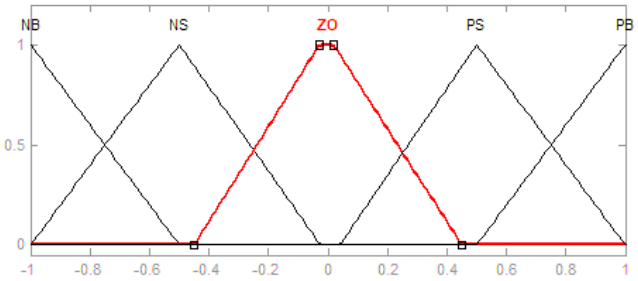


Fig. 7.a. Input membership functions of the SIFLC.

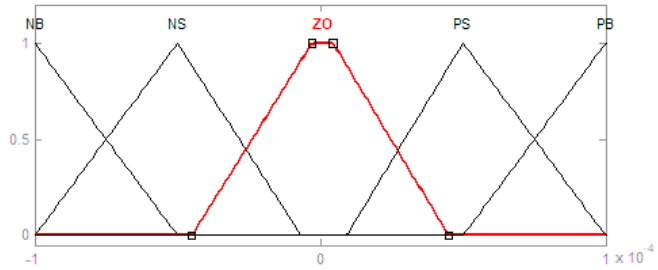
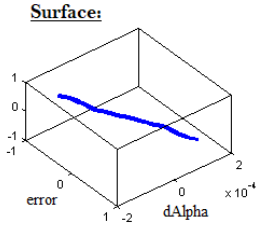


Fig. 7.b. Output membership functions of the SIFLC.

In order to accommodate the 5 rule-based membership functions, the universe of discourse is split into 5 fuzzy sets, each representing a specific linguistic variable in the Fuzzy Logic Controller (FLC). These linguistic variables include Negative Big (NB), Negative Small (NS), Zero (ZO), Positive Small (PS), and Positive Big (PB). The construction of the 5 rules is shown in Fig.8.



Rules :

1. If (error is NB) then (dAlpha is NB)
2. If (error is NS) then (dAlpha is NS)
3. If (error is ZO) then (dAlpha is ZO)
4. If (error is PS) then (dAlpha is PS)
5. If (error is PB) then (dAlpha is PB)

Fig. 8. The SIFLC's chosen rules.

3.2. Speed Estimation

In this section, a Luenberger Observer (LO) is constructed to estimate the DC motor speed in order to replace the mechanical sensor and therefore reducing the overall cost of the proposed system and enhancing its stability against measurement inaccuracies. The idea of using measured data for state estimation has been explored since the initial years of the 1960s. Luenberger focused on the specific challenge of estimating a linear state function, particularly within the domain of single-output linear systems. [16] [17].

In this context, we will first investigate the following linear time-invariant system.

$$\begin{cases} \dot{x}(t) = A.x(t) + B.u(t) \\ y(t) = C.x(t) \end{cases} \quad (6)$$

Under the assumption that the input vector u(t) and output vector y(t) may be measured accurately, and the state variables x(t) are fully observable, the LO can be used to estimate the state variables.

Denoting the estimate of x(t) as $\hat{x}(t)$, the LO can be defined based on the following relations:

$$\begin{cases} \dot{\hat{x}}(t) = A.\hat{x}(t) + B.u(t) + L.(\hat{y}(t) - y(t)) \\ \hat{y}(t) = C.\hat{x}(t) \end{cases} \quad (7)$$

Where $L = [l1 \quad l2]$ is the observer gain matrix, to be selected correctly so that the system is stable. The estimation error is then a consequence of the variance between the measured and the estimated states:

$$\mathrm{e(t)} = \hat{x}(t) - x(t) \quad (8)$$

And with Eqs. 7 and Eqs. 8 it follows that:

$$\dot{e}(t) = [\mathrm{A} - \mathrm{LC}].\mathrm{e(t)} \quad (9)$$

This implies that, regardless of the initial conditions and inputs, the error asymptotically converges to zero as time (t) approaches infinity, provided that the eigenvalues of the gain matrix A-LC are located on the left side of the complex frequency plane.

In our case study, the current and the armature voltage of the DC motor are the only measurable variables available to the state observer. The following equations offer an expression for the dynamic model of the DC motor:

$$\frac{d}{dt}\begin{bmatrix} I_a \\ \omega \end{bmatrix} = \begin{bmatrix} \frac{-R}{L} & \frac{-k}{L} \\ \frac{k}{J} & \frac{f_v}{J} \end{bmatrix} . \begin{bmatrix} I_a \\ \omega \end{bmatrix} + \begin{bmatrix} \frac{1}{L} \\ 0 \end{bmatrix} . V_a \qquad (10)$$

With ω : DC motor speed, L: armature inductance; f_v: coefficient of friction; j: inertia moment; k: torque constant; I_a & V_a: armature current & voltage.

The state variables and gain matrix of the studied system are then given by:

$$x(t) = \begin{bmatrix} I_a \\ \omega \end{bmatrix} ; A = \begin{bmatrix} \frac{-R}{L} & \frac{-k}{L} \\ \frac{k}{J} & \frac{f_v}{J} \end{bmatrix} ; B = \begin{bmatrix} \frac{1}{L} \\ 0 \end{bmatrix} ; C = [1 \quad 0] ;$$

$$u(t) = V_a$$

Fig.8 illustrates the block diagram of the Luenberger speed estimator.

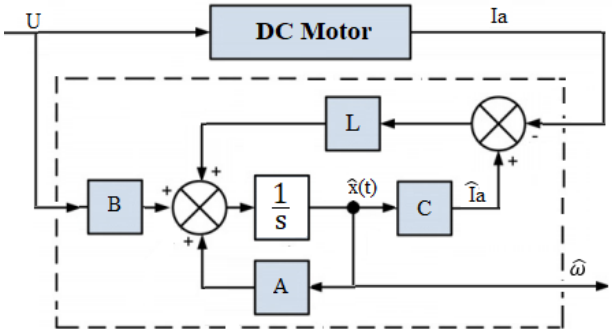


Fig. 9. Block diagram of Luenberger Estimator.

To ensure the gradual disappearance of the estimation error for any initial condition $\hat{X}(0)$ and to guarantee stability across all speed ranges, a common approach consist of picking the observer poles λ_{LO} in proportion to the poles of the DC motor, with a proportionality constant kp ≥ 10.

So if the poles of the DC motor are denoted by λ_{DCM}, the observer poles λ_{LO} can be set as follows:

$$\lambda_{LO} = K_p . \lambda_{DCM} \qquad (11)$$

4. Implementation and Experimental Results

In this section, we have carried out experimental validation for the proposed WTE and the obtained results will be presented. Fig.10 illustrates the various components of the developed bench consisting of:

- A 1.5kW self-excited asynchronous generator mechanically coupled to a 1.5kW, 1500 rpm separate excitation DC motor.
- A DC / DC Boost converter of SEMIKRONTM brand, built around an IGBT 1200V / 50A.
- A PC with a Dspace 1104 card and a command interface to adapt the signals presented or received from the driver of the IGBT (switching order and error signals).
- A measurement interface composed of a voltage sensor, a current sensor and a speed sensor allowing the acquisition of the necessary parameters to control the system.

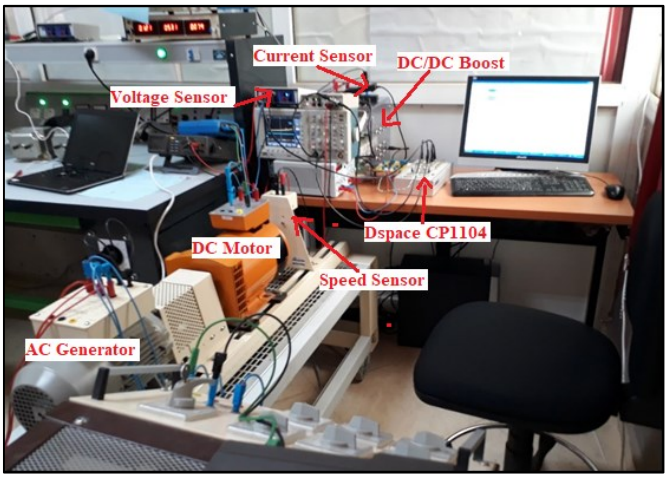


Fig. 10. Wind turbine Emulator test bench.

4.1. Open Loop Validation Tests

The objective of this experimental test is to replicate the mechanical power curves as function of wind turbine rotational speed. To achieve this, the DC-DC boost converter's duty cycle was varied within the 0 to 0.9 range for each designated wind speed value. Fig.11 illustrates results that support the expected behavior of the WTE. The system effectively reproduces the power curves in an open-loop configuration, with each wind speed value corresponding to a distinct maximum point on the power curve.

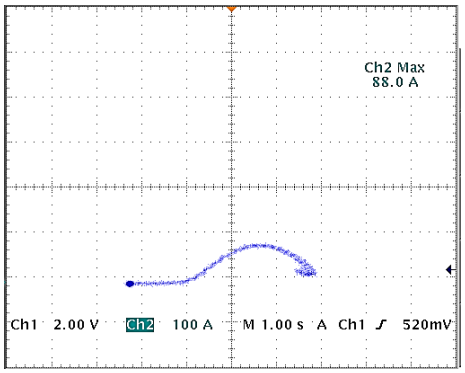


Fig. 11.a. Mechanical power curve at 4.5m/s.

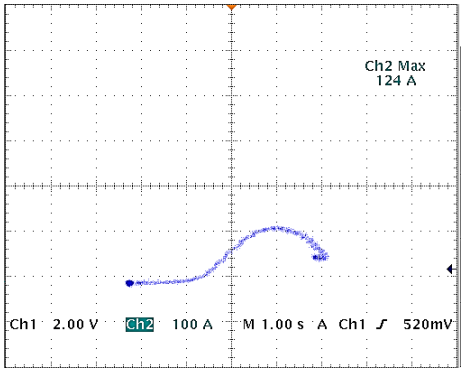


Fig. 11.b. Mechanical power curve at 5m/s.

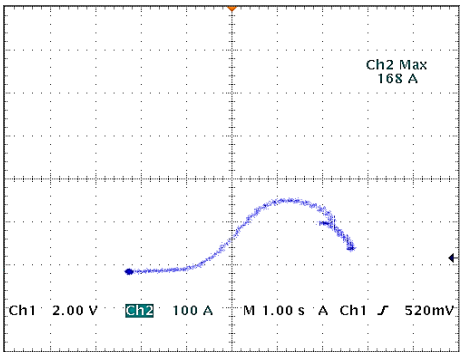


Fig. 11.c. Mechanical power curve at 5.5m/s.

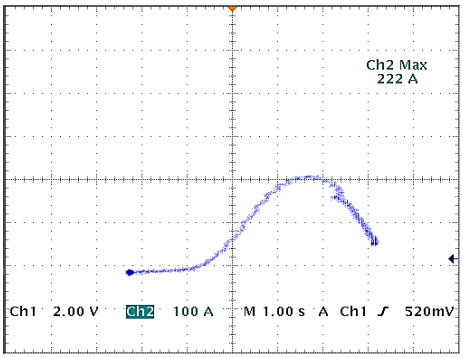


Fig. 11.d. Mechanical power curve at 6m/s.

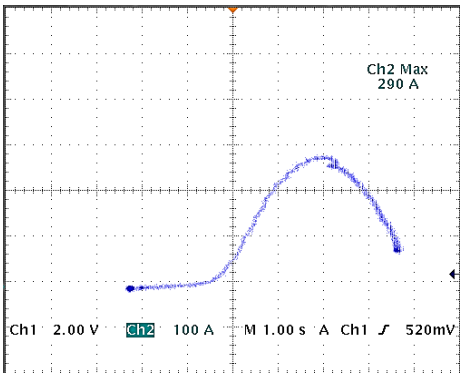


Fig. 11.e. Mechanical power curve at 6.5m/s.

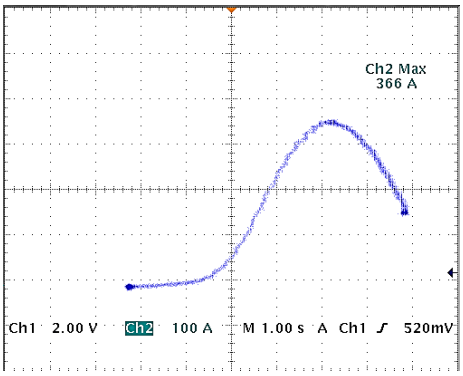


Fig. 11.f. Mechanical power curve at 7m/s.

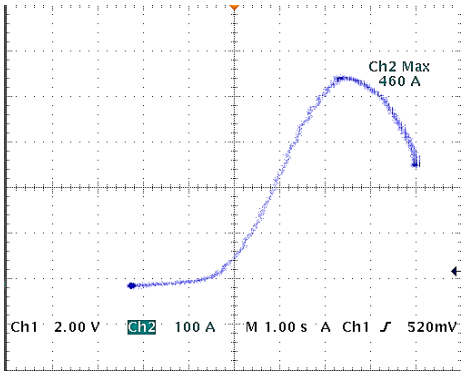


Fig. 11.g. Mechanical power curve at 7.5m/s.

4.2. Speed Observer Validation Tests

To be able to examine the efficiency of the speed observer, a supervision interface was developed with ControlDesk software to provide a friendly user interface allowing modification of certain parameters like wind speed. It also helps real time visualization and data storage of different parameters including rotor speed or measured armature current and voltage.

The operation mode of the entire test bench can be completely controlled through the supervisory interface. Fig.14 displays a screenshot of this interface along with the Simulink block diagram of the proposed control strategy.

In the following, the efficiency of the observer will be examined, and a special attention will be given to understand its behaviour under different working conditions. In the first test, the emulator speed changes from 36 to 76 rad/s with a speed ramp of 7s. While in the second test, a variable speed profile between 36 to 90 rad/s have been chosen.

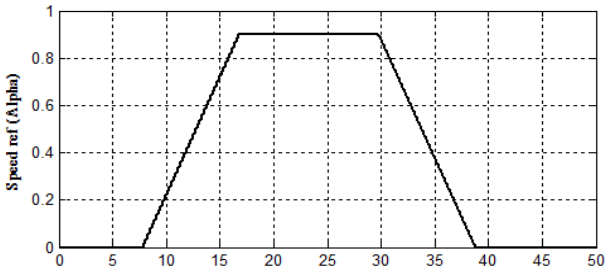


Fig. 12. Speed reference ramp test.

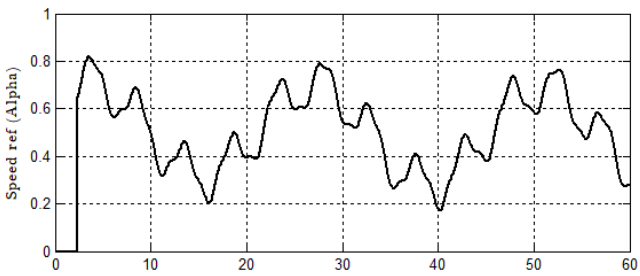


Fig. 13. Speed reference variable test.

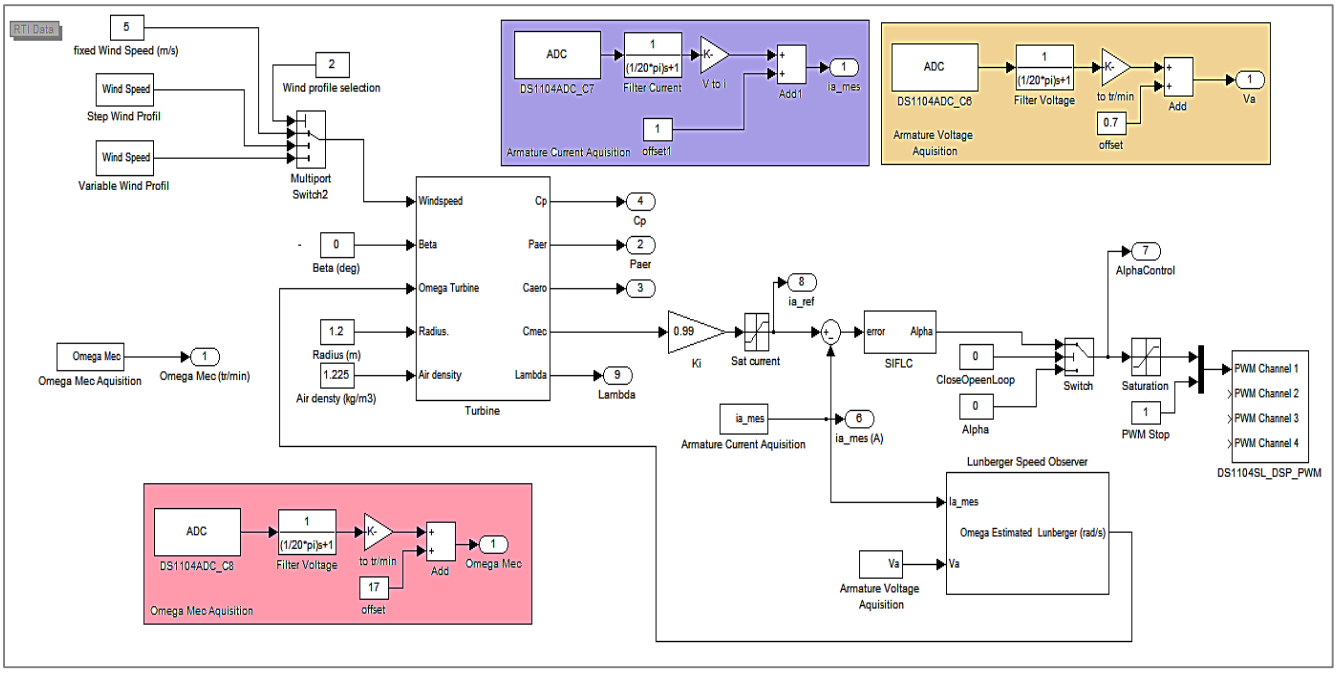


Fig. 14.a. The Simulink block diagram of the proposed control strategy.

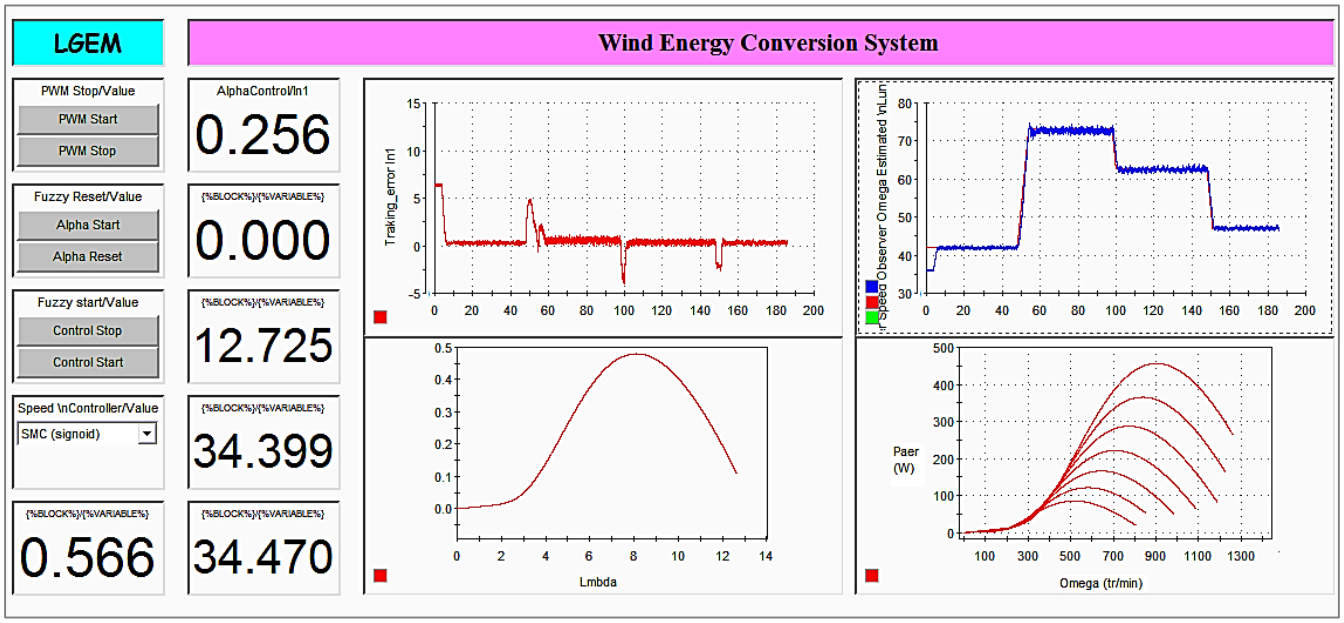


Fig. 14.b. One of the supervision interfaces.

The experimental results displayed in Figs. 15-22 shows that the observer have an excellent tracking performance for speed and current variations at both ramp and variable speed profile.

The studied observer has also presented a precise estimation in transient and steady-state regime with a speed error less than 5% and a current error less than 2%.

The proportionality constant chosen for the pole position of the observer has good effect on its dynamic performances and clear impact on the convergence error of the estimated values.

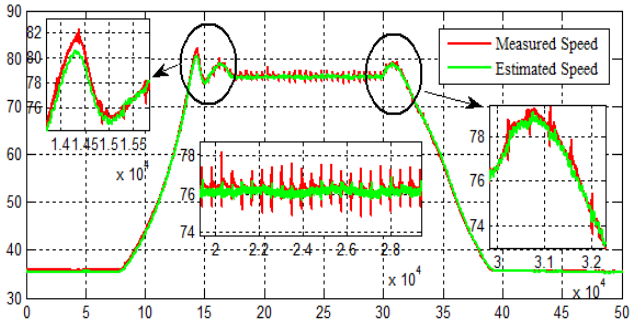


Fig. 15. Estimated and measured speed (rad/s).

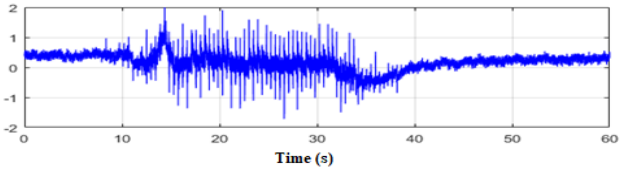


Fig. 16. Estimated error of turbine emulator speed (rad/s).

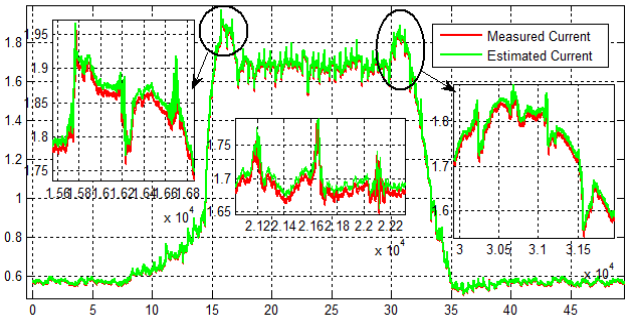


Fig. 17. Measured and Estimated armature current Ia (A).

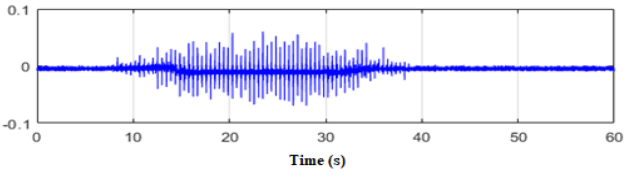


Fig. 18. Estimated error of the armature current (A).

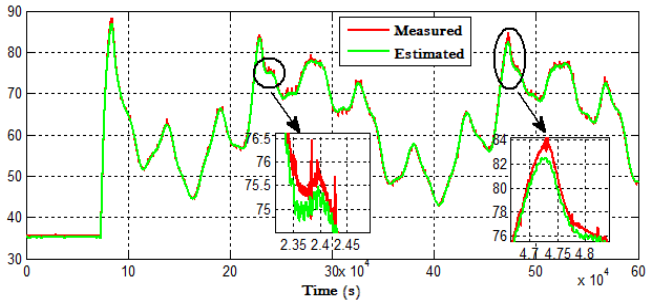


Fig. 19. Estimated and measured speed (rad/s).

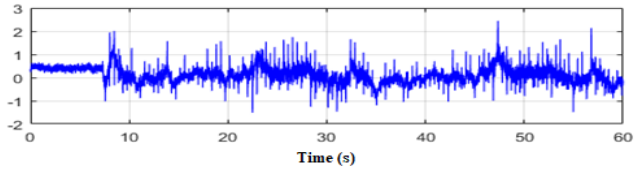


Fig. 20. Estimated error of turbine emulator speed (rad/s).

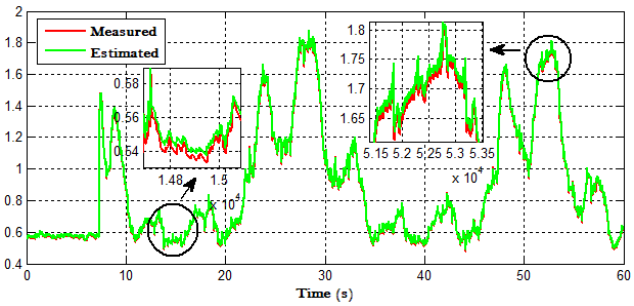


Fig. 21. Measured and estimated armature current Ia (A).

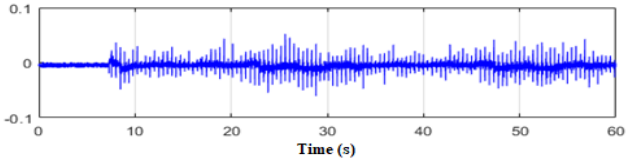


Fig. 22. Estimated error of the armature current (A).

4.3. Closed Loop Validation Tests

Fig.23 illustrates the wind speed signal employed in this experiment. To simulate real-world wind conditions, a pseudorandom wind profile was generated using a series of step changes, with each step ranging between 4 and 6 m/s. While the actual wind profile does not exhibit such abrupt transitions, the use of step-based signals is a common approach in testing, enabling a clear assessment of the system's behavior.

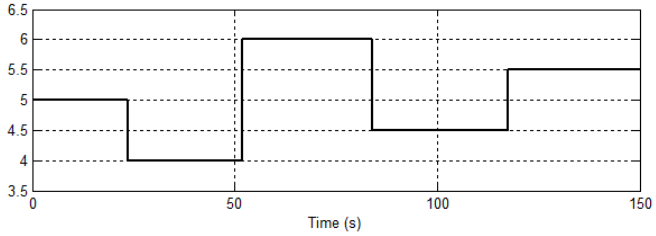


Fig. 23. Wind speed profile.

It is evident from Figs.24 and Figs.25 that the emulator power Paer and shaft speed ω exhibit dynamic responses when subjected to changes in wind speed. These responses gradually converge towards new equilibrium points as the system adjusts to the new operating conditions. For example, as the wind speed transitions from 6m/s to 4.5m/s the emulator power drops from 268.4 W to 107.5 W while the shaft speed decreases from 92 rad/s to 73.35 rad/s.

The power–speed characteristic of the WTE at different wind speed values as recorded during experiments are revealed in Fig.26 and confirm that the created emulator replicates correctly the steady-state characteristics of the selected wind turbine at different wind speed conditions.

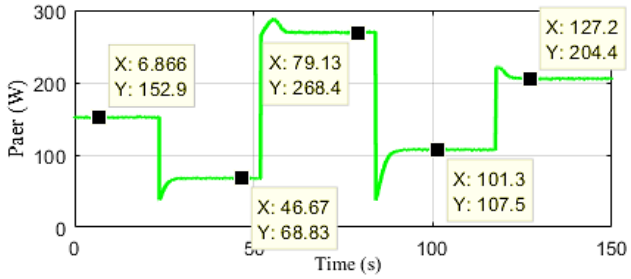


Fig. 24. Paer variations (W).

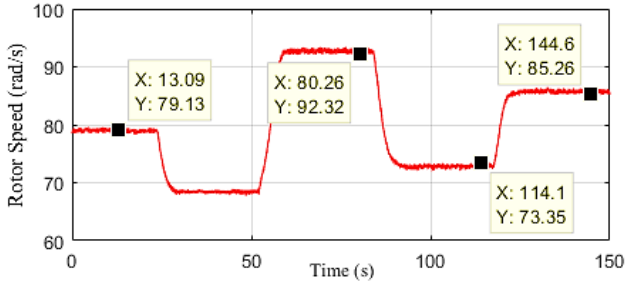


Fig. 25. Emulator Rotor Speed (rad/ s).

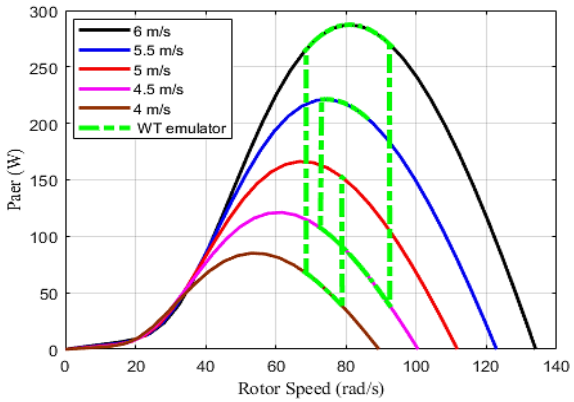


Fig. 26. Paer (W) as function of Omega (rad/s).

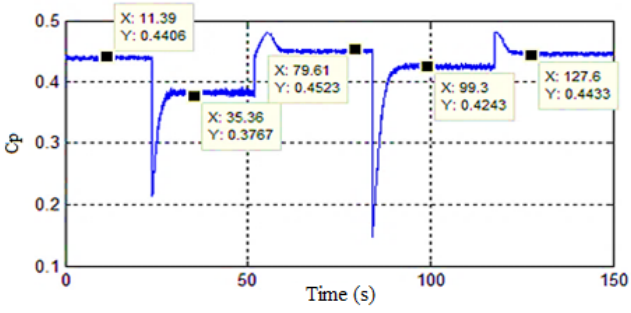


Fig. 27. Power Coefficient Cp.

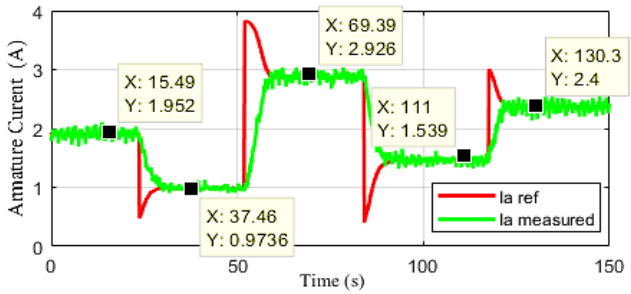


Fig. 28. Armature Current (A).

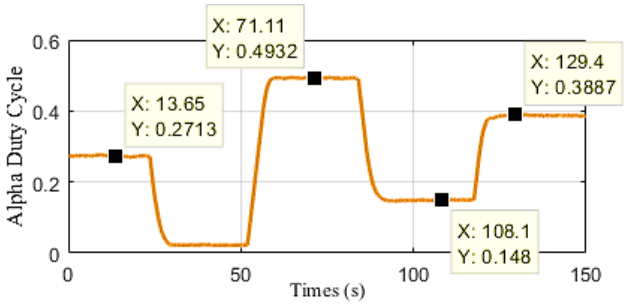


Fig. 29. Alpha duty cycle.

Based on the data shown in Fig.28, it is evident that the measured current (torque) closely follows the fluctuations in the reference current (torque) with no steady-state deviation. This indicates that the proposed SIFLC demonstrates excellent performance in terms of accuracy and fast tracking. One notable advantage of the SIFLC is its simplicity, since it doesn't require knowing the system parameters to calculate the duty cycle Alpha. And as observed in Fig.29 the command signal exhibits no perturbations or noise.

The variation of the power coefficient Cp is in the other hand presented in Fig.27. Experimental observations reveal that the obtained power coefficient values can not reach the theoretical peak of 0.48, as reported by Betz.

5. Conclusion

The unpredictable behavior of the wind and the inherent nonlinearity of wind turbines have been key factors driving research efforts to enhance wind-energy conversion systems. Conducting experimental tests of new control approaches under actual wind conditions is challenging. To overcome such limitations, a low-cost wind turbine was created to replicate the behavior of realistic wind turbines.

This paper has presented a sensorless WTE based on a separately excited DC motor with torque (current) control strategy using a DC/DC boost converter and a single input fuzzy logic controller. The wind turbine model and controller were constructed using the MATLAB/Simulink platform and deployed on the Dspace DS1104 Control Board. This choice facilitated easy accessibility, programming flexibility, and the ability to make modifications as needed. The control software incorporated in the system allows the integration of different wind turbines parameters and wind profiles, enhancing so the experimental capabilities. Furthermore, the ControlDesk software included a supervisor program that provided a user-friendly interface and a variety of helpful tools for efficient experiment management and control.

The experimental results indicate a similarity between the steady-state characteristics of the WTE and the actual WT being studied. The WTE performed as expected and can fulfill the criteria of a laboratory-based wind energy generation system.

References

[1] P. E. Battaiotto, R. J. Mantz, P. F. Puleston, "A wind turbine emulator based on a dual DSP processor system", Control Engineering Practice, DOI: https://doi.org/10.1016/0967-0661(96)00132-3

[2] M. Monfared, H.Kojabadi, H. Rastegar, "Static and dynamic wind turbine simulator using a converter controlled dc motor", Renewable Energy, DOI : https://doi.org/10.1016/j.renene.2007.06.007

[3] R. Ahshan, M. T. Iqbal, G. KI Mann, "Controller for a small induction-generator based wind-turbine", Applied Energy, DOI: https://doi.org/10.1016/j.apenergy.2007.07.005

[4] I. Moussa, A. Bouallegue, A. Khedher, "New wind turbine emulator based on DC machine: hardware implementation using FPGA board for an open-loop operation", IET Circuits, Devices & Systems, DOI: https://doi.org/10.1049/iet-cds.2018.5530

[5] M. El Mokadem, V. Courtecuisse, C. Saudemont, B. Robyns, J. Deuse, "Experimental study of variable speed wind generator contribution to primary frequency control", Renewable Energy, DOI: https://doi.org/10.1016/j.renene.2008.04.033

[6] F. Martinez, L. Carlos Herrero, S. de Pablo, "Open loop wind turbine emulator", Renewable Energy, DOI: https://doi.org/10.1016/j.renene.2013.09.019

[7] S. Tammaruckwattana, O. Kazuhiro, S. Arinaga, "Wind turbine emulator based on blade element momentum theory for variable-speed wind power generation system", IEEJ Transactions on Electrical and Electronic Engineering, DOI: https://doi.org/10.1002/tee.22170

[8] O. Saleem, T. Shami, K. Mahmood-ul-Hasan, "Time-optimal control of DC-DC buck converter using single-input fuzzy augmented fractional-order PI controller", International Transactions on Electrical Energy Systems, DOI: https://doi.org/10.1002/2050-7038.12064

[9] J. Castelló, J. M. Espí, R. García-Gil, "Development details and performance assessment of a wind turbine emulator", Renewable energy, DOI: https://doi.org/10.1016/j.renene.2015.09.010

[10] H. Kojabadi, C. Liuchen, B. Tobie, "Development of a novel wind turbine simulator for wind energy conversion systems using an inverter-controlled induction motor", IEEE Transactions on Energy conversion, DOI: https://doi.org/10.1109/TEC.2004.832070

[11] A. Sajadi, Ł.Rosłaniec, M. Kłos, P. Biczel, K. Loparo, "An emulator for fixed pitch wind turbine studies", Renewable Energy, DOI: https://doi.org/10.1016/j.renene.2015.10.033

[12] J. Yan, Y. Feng, J. Dong, "Study on dynamic characteristic of wind turbine emulator based on PMSM", Renewable Energy, DOI: https://doi.org/10.1016/j.renene.2016.06.034 (Article)

[13] M. E. Abdallah, O. M. Arafa, A. Shaltot, G. A. A. Aziz, "Wind turbine emulation using permanent magnet synchronous motor", Journal of Electrical Systems and Information Technology, DOI: https://doi.org/10.1016/j.jesit.2018.03.005

[14] D. Dolan, " Real-time wind turbine emulator suitable for power quality and dynamic control studies"

[15] S. Tammaruckwattana, K. Ohyama, "Experimental verification of variable speed wind power generation system using permanent magnet synchronous generator by wind turbine emulator", In IECON -38th Annual Conference, DOI: https://doi.org/10.1109/IECON.2012.6389131

[16] Z. Yongchang, Z. Zhengming, "Speed sensorless control for three-level inverter-fed induction motors using an extended Luenberger observer", In 2008 IEEE Vehicle Power and Propulsion Conference, DOI: https://doi.org/10.1109/VPPC.2008.4677412

[17] M. Jouili, K. Jarray, Y. Koubaa, M. Boussak, "Luenberger state observer for speed sensorless ISFOC induction motor drives", Electric Power Systems Research, DOI: https://doi.org/10.1016/j.epsr.2012.02.014

[18] B. J. Choi, S. W. Kwak, B. K. Kim, (1999), "Design of a single-input fuzzy logic controller and its properties", Fuzzy Sets and Systems", DOI: https://doi.org/10.1016/S0165-0114(97)00283-2

[19] M. Farhat, O. Barambones, L. Sbita, "Efficiency optimization of a DSP-based standalone PV system using a stable single input fuzzy logic controller", Renewable and Sustainable Energy Reviews, DOI: https://doi.org/10.1016/j.rser.2015.04.123

[20] A. Dahbi, M. Hachemi, N. Nait-Said, M. S. Nait-Said, "Realization and control of a wind turbine connected to the grid by using PMSG", Energy Conversion and Management, DOI: https://doi.org/10.1016/j.enconman.2014.03.085

[21] N. Hidouri, "An efficiency experimented wind turbine emulator linked to transmission line model 380 kV" Electrical Engineering", DOI: https://doi.org/10.1007/s00202-016-0486-y

[22] Y. A. Eldahab, N. H. Saad, A. Zekry, "Assessing wind energy conversion systems based on newly developed wind turbine emulator.", International Journal of Smart Grid-ijSmartGrid, DOI: https://doi.org/10.13140/RG.2.2.32464.74240

[23] R. Z. Caglayan, K. Kayisli, N. Zhakiyev, A. Harrouz, I. Colak, "A case study: standalone hybrid renewable energy systems", In 11th International Conference on Renewable Energy Research and Application, DOI: https://doi.org/10.1109/ICRERA55966.2022.9922792

[24] O. Alkul, D. Syed, S. Demirbas, "A review of wind energy conversion systems", In 10th International Conference on Smart Grid, DOI:

https://doi.org/10.1109/icSmartGrid55722.2022.9848755

[25] A. Colak, K. Ahmed, "A brief review on capacity sizing, control and energy management in hybrid renewable energy systems", In 10th International conference on renewable energy research and application, DOI: https://doi.org/10.1109/ICRERA52334.2021.9598654